Published in final edited form as:
*J Immunol*. 2009 January 15; 182(2): 1021–1032.

# Ezrin and Moesin Function Together to Promote T Cell Activation[1]

**Meredith H. Shaffer**[*], **Renell S. Dupree**[*], **Peimin Zhu**[†], **Ichiko Saotome**[‡], **Richard F. Schmidt**[*], **Andrea I. McClatchey**[‡], **Bruce D. Freedman**[†], and **Janis K. Burkhardt**[*,2]

[*]Department of Pathology and Laboratory Medicine, Children's Hospital of Philadelphia and University of Pennsylvania, Philadelphia, PA 19104

[†]Department of Pathobiology, University of Pennsylvania School of Veterinary Medicine, Philadelphia, PA 19104

[‡]Massachusetts General Hospital Cancer Center and Harvard Medical School, Department of Pathology, Charlestown, MA 02129

## Abstract

The highly homologous proteins ezrin, radixin, and moesin link proteins to the actin cytoskeleton. The two family members expressed in T cells, ezrin and moesin, are implicated in promoting T cell activation and polarity. To elucidate the contributions of ezrin and moesin, we conducted a systematic analysis of their function during T cell activation. In response to TCR engagement, ezrin and moesin were phosphorylated in parallel at the regulatory threonine, and both proteins ultimately localized to the distal pole complex (DPC). However, ezrin exhibited unique behaviors, including tyrosine phosphorylation and transient localization to the immunological synapse before movement to the DPC. To ask whether these differences reflect unique requirements for ezrin vs moesin in T cell signaling, we generated mice with conditional deletion of ezrin in mature T cells. Ezrin$^{-/-}$ T cells exhibited normal immunological synapse organization based upon localization of protein kinase C-$\theta$, talin, and phospho-ZAP70. DPC localization of CD43 and RhoGDP dissociation inhibitor, as well as the novel DPC protein Src homology region 2 domain-containing phosphatase-1, was also unaffected. However, recruitment of three novel DPC proteins, ezrin binding protein of 50 kDa, Csk binding protein, and the p85 subunit of PI3K was partially perturbed. Biochemical analysis of ezrin$^{-/-}$ T cells or T cells suppressed for moesin using small interfering RNA showed intact early TCR signaling, but diminished levels of IL-2. The defects in IL-2 production were more pronounced in T cells deficient for both ezrin and moesin. These cells also exhibited diminished phospholipase C-$\gamma$1 phosphorylation and calcium flux. We conclude that despite their unique movement and phosphorylation patterns, ezrin and moesin function together to promote T cell activation.

A key feature of T cell activation is polarization with respect to the site of TCR engagement (1–3). Upon recognition of an APC, T cell signaling molecules cluster at the site of cell-cell contact, generating the immunological synapse (IS)[3] (4–7). Protein segregation within the IS

[1]This work was supported by National Institutes of Health Grants R01 AI50098 and P01 CA093615 (to J.K.B.) and by National Institutes of Health Training Grants T32-HD07516-09 and T32-GM7229-29 (to M.H.S.).



[2]Address correspondence and reprint requests to Dr. Janis K. Burkhardt, Department of Pathology and Laboratory Medicine, Children's Hospital of Philadelphia, 816D Abramson Research Center, 3615 Civic Center Boulevard, Philadelphia, PA 19104. jburkhar@mail.med.upenn.edu.

**Disclosures**
The authors have no financial conflict of interest.

is important for the propagation and termination of TCR signaling (6–8). In parallel with IS formation, the distal pole complex (DPC) forms at the opposing pole of the cell. Although comparatively little is known about DPC function, DPC proteins include negative regulators of TCR signaling, and it has been proposed that the DPC promotes T cell activation by sequestering proteins that would inhibit events at the IS (1). In addition, the DPC contains proteins associated with cell polarity in other cell types, and formation of this polarity complex has been implicated in asymmetric segregation of determinants leading to effector and memory T cell fates (9, 10).

Proteins of the ezrin, radixin, and moesin (ERM) family are central regulators of DPC formation. This family of closely related proteins tethers numerous cytoplasmic and transmembrane proteins to F-actin filaments, organizing these cargo molecules into specific regions of the cell cortex (11, 12). T cells express two ERM proteins, ezrin and moesin, both of which localize to the DPC. CD43 and several other DPC proteins have been shown to bind directly to ERM proteins. In the case of CD43, this interaction has been mapped to a cluster of basic residues in the cytoplasmic tail. Mutation of these residues leads to mislocalization of CD43 and defects in T cell activation (13–15). Overexpression of a dominant-negative mutant that disrupts the binding of all ERM proteins to cargo molecules perturbs the localization of CD43 and other proteins to the DPC. This results in diminished cytokine responses, without affecting IS formation or other early T cell activation events (14–16).

ERM function is regulated by intramolecular interactions that mask cargo binding sites within the N-terminal FERM domain, as well as the C-terminal actin binding site (17). Activation is mediated by phosphorylation on a conserved threonine in the actin-binding domain (18–20). In resting T cells, a pool of active ERM proteins is present at the cell cortex in a random distribution. Upon TCR engagement, ERM proteins undergo dephosphorylation, releasing cargo molecules from their cytoskeletal tethers (21, 22). Within minutes, ERM proteins are rephosphorylated, an event that is accompanied by redistribution of ERM proteins and their binding partners to the distal T cell pole (14, 15). Similar events occur in response to chemokine receptor signaling, in which ERM protein dephosphorylation leads to microvillar collapse, thereby promoting the transition from tethering and rolling to integrin-dependent cell-cell adhesion (22–24).

Functional analysis of ERM proteins has been hindered by several problems. First, cells typically contain a large inactive pool, and the active pool can be difficult to solubilize under conditions that preserve protein-protein interactions (12, 25). Second, epitope tagging of ERM proteins disrupts the autoinhibited fold, and active mutants can have toxic effects (17). Finally, ERM proteins exhibit high sequence homology (>70% amino acid identity). They migrate together by SDS-PAGE unless care is taken to resolve them, and many Abs cross-react. Most cargo proteins bind to multiple ERM proteins. Because many cell types express two or more ERM family members, they are widely considered to be functionally redundant. In support of this idea, moesin-deficient mice were found to be viable and grossly normal (26). Thus, most studies have used dominant-negative mutants that interfere functionally with all ERM proteins. Although these mutants are very useful, they can cause off-target effects by interfering with actin dynamics or with other FERM-domain-containing proteins. Moreover, they cannot be used to address the roles of individual ERM proteins.

[3]Abbreviations used in this paper: IS, immunological synapse; DPC, distal pole complex; ERM, ezrin, radixin, and moesin; MCC, moth cytochrome *c*; PKC, protein kinase C; PLC, phospholipase C; SH2, Src homology 2; SHP-1, Src homology region 2 domain-containing phosphatase-1; shRNA, short hairpin RNA; siRNA, small interfering RNA; Tg, transgenic; CBP/PAG, Csk binding protein/phosphoprotein associated with glycosphingolipid-enriched microdomain.

A number of recent reports suggest that ERM proteins play unique roles in some contexts. Radixin-deficient mice have hyper-bilirubinemia due to defects in the liver (27). Ezrin-deficient mice exhibit perinatal lethality due to defects in the gut epithelium (28). These mice also show defects in retinal pigment epithelial cells (29). To date, the dramatic defects reported in mice lacking single ERM proteins are all found in cell types in which only one ERM protein is expressed at appreciable levels. Recently, Bretscher and colleagues (30) reported that overexpression of ezrin mutants or small interfering RNA (siRNA)-mediated suppression of ezrin in T cells disrupts key signaling events, including IS formation, ZAP70 localization, and $Ca^{2+}$ flux. Because T cells express both ezrin and moesin, with moesin the more abundant family member (31), this study argues that ezrin is specifically required for certain aspects of T cell activation, and that moesin cannot substitute for ezrin in this context.

Using a mouse model with conditional deletion of ezrin in T cells, in combination with siRNA suppression of moesin, we have conducted a systematic analysis of the individual and overlapping functions of ERM proteins in TCR signaling. We demonstrate that ezrin and moesin show distinct behaviors in T cells. However, we could find no aspects of TCR signaling that uniquely required ezrin or moesin. Instead, T cell activation appears to depend on net ERM protein expression.

## Materials and Methods

### Mice

Mice homozygous for a floxed ezrin gene (28) were crossed with CD4-Cre transgenic (Tg) mice on the C57BL/6 background (Taconic Farms) to generate mice with deletion of ezrin late in T cell development. For some studies, $Ezrin^{flox/flox}$ and CD4-Cre mice were also bred to mice bearing the AND TCR transgene (Jackson ImmunoResearch Laboratories) to generate T cells specific for moth cytochrome *c* $(MCC)_{88–103}$ presented on $I\text{-}E^k$ (32). Tg mice used for experiments were bred to have only one copy of the AND transgene. Wild-type littermates were used as controls. C57BL/6 mice were obtained from Jackson ImmunoResearch Laboratories. All mice were housed in the Children's Hospital of Philadelphia animal facility, according to guidelines put forth by the Institutional Animal Care and Use Committee.

### Cell culture

All tissue culture reagents were from Invitrogen. The human T cell line Jurkat E6.1 was maintained in RPMI 1640 supplemented with 5% FBS, 5% newborn calf serum, penicillin, streptomycin, and GlutaMAX. The 293T cells and CH27 B cells were maintained using DMEM supplemented with 10% FBS, nonessential amino acids, penicillin, streptomycin, and 25 mM HEPES. Murine $CD4^+$ lymph node T cells were isolated by negative selection using a mixture of anti-MHC class II (M5/114.15.2) and anti-CD8 (2.43), followed by magnetic bead-conjugated goat anti-rat Ig (Qiagen). Labeled cells were removed using magnetic separation. To generate T-depleted splenocytes, red cells were removed from single-cell suspensions by hypotonic lysis. Cells were washed and subjected to complement-mediated lysis using anti-Thy1.2 (J1j.10) hybridoma supernatant. Dead cells were removed by centrifugation over Histopaque (Sigma-Aldrich). Cells were maintained using DMEM supplemented with 5% FBS, nonessential amino acids, penicillin, streptomycin, HEPES, and 2-ME (Sigma-Aldrich).

### RNA interference

Two siRNA duplexes against murine moesin were synthesized by Dharmacon. The following targeting sequences were used: siMoesin no. 1, GGAGCGUGCUCUCCUGGAA

and siMoesin no. 2, CGGUCCUGUUG GCUUCUUA. Experiments shown were performed using siMoesin no. 1, and repeated with siMoesin no. 2 to control for off-target effects. For non-suppressed controls, cells were transfected with siControl no. 2, specific for firefly luciferase (Dharmacon). To generate moesin-deficient murine T cell blasts, freshly isolated ezrin$^{+/+}$ or ezrin$^{-/-}$ CD4$^{+}$ T cells were stimulated in 24-well plates coated with 1 $\mu$g/ml anti-CD3 (2C11) and anti-CD28 (PV-1) in PBS, and cultured for 3 days at 37°C, 10% $CO_2$. Two days after removal from anti-CD3/anti-CD28, cells were washed and resuspended in unsupplemented DMEM. Cells ($10^7$) were mixed with 500 pmol siRNA duplexes in a 4-mm gap cuvette, and transfected using a BTX electroporator at 290V for 10 ms. After transfection, cells were maintained in complete DMEM with 100 U/ml human rIL-2 (obtained through the AIDS Research and Reference Reagent Program, Division of AIDS, National Institute of Allergy and Infectious Diseases, National Institutes of Health; human rIL-2 from M. Gately, Hoffmann-LaRoche, Nutley, NJ). Cells were assayed 48–72 h posttransfection.

For studies in Jurkat T cells, knockdown oligos were synthesized and cloned into pCMS3.eGFP.H1p, as described previously (33). The following targeting sequences were used: shEzrin no. 1, CCAATCAATGTC CGAGTTA; shEzrin no. 2, CCGTGGAGAGAGAGAAAGA; shMoesin no. 1, GCAGCGCATTGACGAATTT; and shMoesin no. 2, GGAGCGT CAAGAAGCTGAA. Short hairpin RNA (shRNA) vectors were transfected by electroporation, as described (33), and cells were assayed at 72 h after transfection. Analysis of GFP$^{+}$ cells by flow cytometry showed >95% transfection efficiency, and analysis by Western blotting showed ≥80% protein suppression in the bulk population of cells (data not shown and Fig. 8*F*).

## Flow cytometry

Single-cell suspensions were stained with the following fluorescently conjugated mAbs: CD3-PE, CD4-allophycocyanin, CD4-FITC, CD8-PECy7, CD8-allophycocyanin, CD25-PE, CD69-PE, B220-PE, CD62L-PE, CD44-FITC, or IgM-FITC (Biolegend). Intracellular labeling with rabbit anti-ezrin (Cell Signaling Technology), followed by AlexaFluor488 goat anti-rabbit (Invitrogen) or AlexaFluor488-conjugated anti-FoxP3 (Biolegend), was performed as per manufacturer's instructions. Flow cytometry was performed on a FACSCalibur (BD Biosciences), and analysis was done using FlowJo (Tree Star). Dead cells were excluded based on forward scatter/side scatter analysis.

## Functional studies

Stimulations for analysis of activation marker expression, IL-2 production, and proliferation were done in parallel. Ezrin- and/or moesin-deficient T cells ($2 \times 10^5$) and T cell-depleted splenocytes ($5 \times 10^4$) were cocultured in 96-well plates in the presence of the indicated concentrations of anti-CD3, in a total of 200 $\mu$l. Alternatively, cells were stimulated with plate-bound anti-CD3 and anti-CD28 Abs (1 $\mu$g/ml). Each stimulation condition was set up in quadruplicate. Supernatants were removed at 24 h and stored at −80°C until analysis of IL-2 by ELISA (eBioscience). For some ELISA studies, cells and supernatants were lysed together, with similar results. For proliferation analysis, cells were loaded with CFSE (Invitrogen) before stimulation. To assay up-regulation of CD25 and CD69 and down-regulation of CD3, the cells were harvested at 24 h, washed, and labeled with appropriate Abs for analysis by flow cytometry. For $Ca^{2+}$ imaging of single cells, mouse or Jurkat T cells were loaded with the cell-permeant $Ca^{2+}$ indicator fura 2-AM (3.0 $\mu$M; Invitrogen). $Ca^{2+}$ mobilization was measured, as previously described (34).

For analysis of transcriptional activation, Jurkat T cells were transfected with 20 $\mu$g of each suppression vector, or 40 $\mu$g of empty suppression vector, together with 5 $\mu$g of the

indicated luciferase reporter plasmid (NF-AT/AP-1 LUC or NF-κB-LUC, gift from D. McKean, Mayo Clinic, Rochester, MN) and 20 ng of a TK-*Renilla* reporter plasmid (Promega). After 72 h, $1 \times 10^5$ cells were distributed into 96-well culture plates and stimulated for 7 h with $1 \times 10^5$ Raji B cells ± 300 ng/ml staphylococcal enterotoxin E (Toxin Technology). Samples were lysed and assayed on a Berthold LB960 Plate luminometer using the Dual Luciferase Assay kit (Promega), and normalized for *Renilla* activity. Data represent average ± SD of quadruplicate samples, from one representative experiment (from a total of three); statistical significance was calculated using a paired Student's *t* test.

## Biochemical analysis of T cell activation

Naive purified T cells or T cell blasts were collected and resuspended in either RPMI 1640 containing 1% FBS or serum-free DMEM for chemokine stimulation or TCR stimulation, respectively. For chemokine stimulations, CCL19 was added at 250 μg/ml, and cells were incubated at 37°C for the indicated times. For TCR cross-linking, cells were rested on ice and labeled with 10 μg/ml biotinlyated anti-CD3 Ab (Biolegend). Stimulation was initiated by the addition of streptavidin (20 μg/ml). For vanadate treatment, equal parts 100 mM $Na_3VO_3$ and 3% $H_2O_2$ were mixed and allowed to react at 25°C for 10 min. Vanadate was added to T cells using a 1/33 dilution. Cells were incubated at 37°C, removed at indicated times, and lysed using TTX lysis buffer (1% Triton X-100, 50 mM Tris-HCl (pH 8.0), 50 mM NaCl, 5 mM EDTA, 50 mM NaF, protease inhibitors, and 1 mM $NaVO_4$). Insoluble material was pelleted at 13,000 rpm for 20 min. Protein concentrations were determined using a bicinchoninic acid assay (Pierce). For immunoprecipitation of tyrosine-phosphorylated proteins, a mixture comprised of PT66-agarose (Sigma-Aldrich), PY69-agarose (BD Biosciences), PY99-agarose (Santa Cruz Biotechnology), PY-Sepharose 4B (Zymed Laboratories), and 4G10-agarose (Upstate Biotechnology) was prepared and incubated with lysates from $40 \times 10^6$ mouse T cells. After washing with TTX lysis buffer, beads were boiled in sample buffer and separation was performed using SDS-PAGE electrophoresis on Tris-glycine gels with 10% acrylamide. Proteins were transferred to nitrocellulose and blocked in 3% BSA in PBS. Blots were probed with Abs specific for phosphotyrosine, total ERM, pT-ERM (recognizes pT567 in ezrin, pT558 in moesin), ezrin-pY353, ezrin, moesin, pERK1/2 T202/Y204, pAkt326, pPLC-γY783, pLckY505, pZAP70 Y319 (Cell Signaling Technology), or ezrin pY146 (Santa Cruz Biotechnology), in 3% BSA in TBST. Blots were probed with IR800 goat anti-rabbit Ig (Rockland) or AlexaFluor680 donkey anti-mouse Ig (Invitrogen), and visualized using the Odyssey Imager (LI-COR).

Pull-down studies were performed using a panel of Src homology 2 (SH2) domains (gift from D. Billadeau, Mayo Clinic, Rochester, MN), essentially as described previously (33). Briefly, Jurkat T cells were treated with C305 and pervanadate to promote tyrosine phosphorylation. Whole-cell lysates were incubated with purified rGST-tagged SH2 domains, and bound proteins were detected using anti-ERM Ab.

## Immunofluorescence microscopy

Sulfate latex beads, 5 or 10 μm diameter (Invitrogen), were coated with anti-CD28 alone or together with anti-TCRβ, and mixed with T cells in a 2:1 ratio (beads:cells). Alternatively, for studies using AND Tg T cells, CH27 B cells were stained with CellTracker Blue (Invitrogen) and pulsed with 5 μM $MCC_{88–103}$ peptide. Conjugates were allowed to interact at 37°C for the indicated times, during which they were plated on poly(L-lysine)-coated cover-slips. Cells were fixed in 3% paraformaldehyde in PBS and processed for intracellular immunofluorescence, as described previously (35), using Abs to the indicated proteins (talin, protein kinase C (PKC)-θ, pY390 ZAP70, RhoGDI (all from Santa Cruz Biotechnology), CD43 (BD Pharmingen), EBP50 (Affinity BioReagents), Csk binding

protein/phosphoprotein associated with glycosphingolipid-enriched microdomains (CBP/PAG) (gift from B. Schraven, Ottovon-Guericke University, Magdeburg, Germany), and p85 (gift from M. Birnbaum, University of Pennsylvania School of Medicine, Philadelphia, PA)) or AlexaFluor594-phalloidin or rhodamine-phalloidin (Invitrogen) to label actin filaments. Cells were imaged on an Axiovert 200M microscope (Zeiss) using a ×63 1.4 N.A. Planapo objective. Images were collected using a Coolsnap FX-HQ camera (Roper Scientific), and deconvolution and three-dimensional rendering were performed using Slidebook v4.0 software (3I). Quantitation was performed by randomly selecting conjugates containing a T cell contacting a latex bead or blue-dyed B cell. Localization to the IS was defined by the presence of a distinct band at the cell-cell contact site. Localization to the DPC was defined as exclusion of the protein of interest from the cell-cell contact site or as capping at the T cell pole opposite the site of TCR engagement. Wherever possible, analysis was performed by an individual blinded to experimental conditions. At least 50 conjugates were scored in each of three experiments. Data represent average ± SD; statistical significance was calculated using a paired Student's *t* test.

## Results

### Ezrin, but not moesin, transiently visits the IS

As a first step toward asking whether ezrin and moesin exhibit distinct functions in T cells, we conducted a comparative analysis of the localization of these proteins during T cell activation. Freshly isolated murine $CD4^+$ T cells were stimulated for various times before fixation, and the localization of ezrin and moesin was assessed by fluorescence microscopy. Because all APCs tested expressed high levels of ezrin or moesin, complicating analysis of T cell responses, latex beads coated with anti-TCR$\beta$ and anti-CD28 Abs were used as surrogate APCs. As we observed previously (15), ezrin and moesin colocalized at the DPC when observed 20 min after TCR engagement. However, at early times after cell stimulation, ezrin localized to the IS, whereas moesin localized to the DPC (Fig. 1, *A* and *B*). Quantitative analysis of ezrin and moesin localization at various times after T cell-bead mixing revealed that ezrin transiently visits the IS before localizing to the DPC, whereas moesin immediately travels to the DPC and remains there at later times (Fig. 1, *C*–*F*). This result shows that ezrin and moesin movement with respect to the IS and DPC is differentially controlled.

### Ezrin and moesin differ with respect to tyrosine phosphorylation

Concomitant with movement toward the DPC, ERM proteins undergo transient dephosphorylation on a regulatory threonine (14, 21, 22). A recent study in Jurkat T cells suggests that ezrin and moesin exhibit distinct patterns of threonine dephosphorylation (30), but this was not noted in previous studies (21, 22). To assess threonine phosphorylation patterns in primary T cells, $CD4^+$ murine T cells were stimulated by TCR cross-linking, and lysates were immunoblotted with an Ab that recognizes the conserved phospho-threonine residue using a fluorescence-based detection system to insure linearity of signal. Because chemokine stimulation also induces transient dephosphorylation of ERM proteins (21), similar studies were conducted by stimulating cells with the T cell homing chemokine CCL19. As shown in Fig. 2, *A* and *B*, we observed similar ratios of threonine-phosphorylated ezrin and moesin at each time point in T cells responding to either TCR engagement or chemokines, suggesting that both proteins are dephosphorylated/rephosphorylated at the regulatory threonine by a similar mechanism.

In addition to threonine phosphorylation, ezrin is also tyrosine phosphorylated after TCR stimulation (36). To determine whether ezrin and moesin are differentially tyrosine phosphorylated, lysates from resting and stimulated $CD4^+$ T cells were immunoprecipitated

with a mixture of phosphotyrosine-specific Abs, and eluates were immunoblotted with an Ab that recognizes all ERM proteins. Only ezrin was detected (Fig. 2*C*), indicating that ezrin and moesin differ with respect to tyrosine phosphorylation during T cell activation. As reported previously (36), tyrosine phosphorylation of ezrin was only seen in the presence of the phosphatase inhibitor vanadate, suggesting high turnover of ezrin phosphorylation.

Tyrosines 146 and 353 have been identified as important tyrosine phosphorylation sites on ezrin in other cell types (37–40). To ask whether these sites are phosphorylated in T cells, lysates from resting and activated primary $CD4^+$ T cells were probed with phospho-specific Abs. As shown in Fig. 2*D*, phosphorylation at both tyrosines 146 and 353 could be detected in vanadate-treated cells, and increased phosphorylation was seen with additional CD3 cross-linking. Interestingly, although Y146 is conserved in both ezrin and moesin, Y353 is unique to ezrin, highlighting another difference between these proteins.

As a first step toward defining the functional consequences of ezrin tyrosine phosphorylation, we asked using a GST-pulldown approach whether ERM proteins interact differentially with SH2 domains of several proteins involved in signaling events at the IS. As shown in Fig. 2*E*, the SH2 domain of Lck associated with ezrin, but not moesin, from activated Jurkat T cell lysates. Additional study will be needed to ask whether ezrin binds Lck in vivo, and to test the functional consequences of this interaction. Nonetheless, these data show that tyrosine phosphorylation of ezrin has the potential to generate binding sites for SH2 domain-containing proteins that do not interact with moesin.

## Conditional deletion of ezrin in T cells

Because ezrin and moesin show distinct patterns of movement and phosphorylation during T cell activation, we sought to identify aspects of the T cell response that uniquely depend on ezrin. Mice with germline deletion of ezrin die within a few days of birth (28), making them unsuitable for studies of T cells. We therefore generated conditional ezrin knockouts by crossing $ezrin^{flox/flox}$ mice to mice bearing a CD4-Cre transgene, which mediates excision during the $CD4^+CD8^+$ double-positive stage, late in T cell development (41). $Ezrin^{flox/flox:CD4Cre}$ mice were born in expected Mendelian ratios, and the spleen, thymus, and lymph nodes exhibited normal cellularity (data not shown). As expected, loss of ezrin expression was first detectable in double-positive T cells (Fig. 3*A*). Deletion of ezrin was restricted to the T cell compartment, and ezrin levels in mature single-positive T cells were less than 5% of wild-type levels (Fig. 3*B*). Moesin levels were slightly (10–20%) elevated in naive T cells from some $ezrin^{flox/flox:CD4Cre}$ mice (Fig. 3*B* and data not shown). To determine whether ezrin expression affects T cell development, we next analyzed the percentages of T cell subsets in the thymus and periphery. As shown in Fig. 3*C*, thymocyte populations were similar in wild-type and $ezrin^{flox/flox:CD4Cre}$ mice, indicating that T cell development proceeds normally. Analysis of peripheral lymphoid organs showed no significant differences in CD4/CD8 ratios, or in naive ($CD62L^{high}CD44^{low}$), memory ($CD62L^{low}CD44^{high}$), activated ($CD69^{high}$), or regulatory ($CD4^+CD25^+Foxp3^+$) T cell subsets (Fig. 3*C* and data not shown). Thus, these mice represent a suitable source of mature ezrin-deficient T cells for functional studies. Henceforth, we will refer to mature T cells from $ezrin^{flox/flox:CD4Cre}$ and control $ezrin^{flox/flox}$ mice as $ezrin^{-/-}$ and $ezrin^{+/+}$ T cells, respectively.

## Ezrin$^{-/-}$ T cells have decreased IL-2 production, but early TCR signaling events occur normally

To assess the role of ezrin in T cell activation, purified $ezrin^{+/+}$ and $ezrin^{-/-}$ $CD4^+$ T cells were stimulated by CD3 cross-linking, and patterns of phosphorylation were assessed by Western blot analysis. No defects were observed in total phosphotyrosine patterns or in

phosphorylation of specific signaling molecules, including pPLC-$\gamma$1, pERK, pZAP70, pAkt, and pLck (Fig. 4, *A* and *B*, and data not shown). To assess activation marker expression, cells were stimulated overnight with 0.1 or 1 $\mu$g/ml anti-CD3 plus wild-type T-depleted splenic APCs, and analyzed by flow cytometry. No differences were observed in the number of cells responding or the degree of up-regulation of CD69 and CD25, or in the down-regulation of TCR at either dose (Fig. 4*C* and data not shown). Interestingly, although these early aspects of T cell activation were grossly normal, ezrin$^{-/-}$ T cells showed significant defects in IL-2 production under the same stimulation conditions (Fig. 4*D*). These findings suggest that ezrin is dispensable for early T cell signaling events, but does play a role in downstream events required for efficient IL-2 production.

## IS formation proceeds normally in ezrin$^{-/-}$ T cells, but DPC formation is partially perturbed

A recent study reports that ezrin suppression leads to defects in localization of ZAP70 to the IS (30). Thus, we tested IS formation in ezrin$^{-/-}$ T cells responding to Ag-loaded APCs. To generate Ag-specific T cells deficient for ezrin, ezrin$^{flox/flox}$ or ezrin$^{flox/flox:CD4Cre}$ mice were crossed to mice bearing the AND TCR transgene. Conditional deletion of ezrin occurred efficiently on the AND Tg background, and had no effect on T cell populations or TCR expression levels (data not shown). Purified CD4$^{+}$ T cells from these mice were conjugated to MCC$_{88–103}$-pulsed CH27 B cells, and T/B conjugates were visualized by immunofluorescence microscopy to assess IS formation. Conjugates were analyzed at 3 min after cell mixing, a time when ezrin localizes to the IS. As shown in Fig. 5, *A* and *B*, the canonical IS markers PCK-$\theta$ and talin localized to the IS with similar frequency in conjugates formed with ezrin$^{+/+}$ or ezrin$^{-/-}$ T cells, and these proteins segregated into the peripheral and central supramolecular activation cluster domains associated with productive T cell activation. F-actin responses at the IS were also normal (Fig. 5*B* and data not shown). Although we attempted to visualize the total pool of ZAP70, none of the Abs we tested specifically detected murine ZAP70 in aldehyde-fixed cells. However, we could readily detect the phosphorylated, active pool of ZAP70. As previously reported in wild-type cells (42), IS accumulation of pY319ZAP70 was transient, and was detectable in 20–30% of conjugates at early times after T cell-APC contact. We observed no difference in pZAP70 localization between ezrin$^{+/+}$ and ezrin$^{-/-}$ T cells, indicating that ezrin is not required for recruitment and activation of ZAP70 at the IS (Fig. 5, *C* and *D*).

In our previous studies using the ERM dominant-negative mutant, IS organization was normal, but we observed clear defects in organization of the DPC (16). To test for ezrin-specific effects on DPC formation, ezrin$^{+/+}$ and ezrin$^{-/-}$ T cells were conjugated to anti-TCR$\beta$/CD28 Ab-coated beads, and the distribution of DPC components was assessed. As expected, moesin was recruited to the DPC at similar frequencies in ezrin$^{+/+}$ and ezrin$^{-/-}$ cells, as were CD43 and RhoGDI, proteins thought to bind both ezrin and moesin (Fig. 6, *A–C*) (13, 43). We recently identified the tyrosine phosphatase Src homology region 2 domain-containing phosphatase-1 (SHP-1) as a novel DPC component (Fig. 6*D*). Like CD43 and RhoGDI, SHP-1 distribution was unperturbed in ezrin$^{-/-}$ T cells. We next examined the distribution of CBP/PAG, EBP50, and p85. Each of these proteins has been reported to interact preferentially with ezrin (37, 44), but their localization with respect to the DPC has not been tested. As shown in Fig. 6, *E–G*, CBP/PAG, EBP50, and p85 were each enriched at the DPC in conjugates formed with wild-type T cells. Quantitative analysis showed that these proteins localized to the DPC at similar frequencies as other known DPC components. Ezrin$^{-/-}$ T cells showed diminished DPC localization of each of these proteins; however, this effect was subtle; a significant proportion of conjugates retained DPC localization. This finding supports the idea that some DPC proteins preferentially associate with ezrin, but also

points to the existence of alternate mechanisms that facilitate the movement of these proteins to the DPC.

## Generation of T cells deficient for both ezrin and moesin

The simplest explanation for the modest defects in ezrin$^{-/-}$ T cells is that moesin also contributes to TCR signaling. To test this idea, ezrin$^{+/+}$ or ezrin$^{-/-}$ T cell blasts were transfected with moesin-specific siRNA or control nontargeting oligonucleotides to generate moesin-deficient (Ez$^{+/+}$Mo$^{siM}$), ezrin-deficient (Ez$^{-/-}$Mo$^{siC}$), ezrin/moesin double-deficient (Ez$^{-/-}$Mo$^{siM}$), or control (Ez$^{+/+}$Mo$^{siC}$) T cells. Although we show data generated with a single moesin-specific siRNA, experiments were verified using an independent oligonucleotide (data not shown). To test specificity of the moesin-specific siRNA, T cells were immunoblotted with an Ab that recognizes all ERM proteins, and protein expression was analyzed. By 48 h, moesin levels were reduced by ≥80% relative to control transfectants or mock-transfected cells, without diminution of ezrin expression (Fig. 7*A* and data not shown). We observed no compensatory up-regulation of ezrin protein levels in moesin-suppressed cells, although modest up-regulation of moesin protein levels was sometimes observed in ezrin$^{-/-}$ T cell blasts. Although expression levels varied, moesin-suppressed T cells generally retained about half the normal complement of ERM proteins; ezrin$^{-/-}$ T cells retained slightly more than half; and T cells deficient for both ezrin and moesin retained ~15% of the normal complement of total ERM proteins.

Using these cells, we tested the effects of depletion of both ezrin and moesin on formation of the IS and the DPC. As shown in Fig. 7*B*, Ez$^{-/-}$Mo$^{siM}$ T cells showed normal IS formation, as measured by recruitment of pZAP70, talin, and PKC-$\theta$. This confirms our results using the ERM dominant-negative mutant (16). Surprisingly, however, DPC formation, as measured by recruitment of CD43, also occurred normally. It seems likely that the residual moesin expressed in these cells is sufficient to mediate CD43 targeting to the DPC. In support of this idea, we found that whereas only ~15% of total ERM proteins remained in the double-deficient cells, this pool was hyperphosphorylated on the activating threonine residue (Fig. 7*C*). Thus, these cells retained ~50% of the normal complement of active, phosphorylated ERM proteins.

## Ezrin and moesin each contribute to IL-2 production

Despite the fact that the double-deficient cells retain significant levels of active ERM proteins, these cells demonstrated functional defects. As shown in Fig. 8*A*, ezrin$^{-/-}$ T cell blasts produced lower levels of IL-2 than control cells, consistent with the defects observed in naive ezrin$^{-/-}$ T cells (Fig. 4*D*). Moesin-deficient T cell blasts also exhibited reduced IL-2 production, and T cells deficient for both ezrin and moesin expressed the lowest levels of IL-2 (Fig. 8*A*).

## Both ezrin and moesin are required for optimal $Ca^{2+}$ flux and phospholipase C (PLC)-γ1 activation

To analyze events upstream of IL-2 production, ezrin- and/or moesin-deficient cells were stimulated with anti-CD3 Ab, and the activation of key signaling intermediates was assessed by Western blotting with phospho-specific Abs. As shown in Fig. 8*B*, T cell blasts deficient for either ezrin or moesin alone showed no obvious defects in phosphorylation of PLC-$\gamma$1, ZAP70, or ERK1/2. Like the single-deficient cells, T cells deficient for both ezrin and moesin showed normal phosphorylation of ERK1/2, but the double-deficient T cells consistently showed diminished phosphorylation of PLC-$\gamma$1. In some cases, defects in ZAP70 phosphorylation could also be detected (Fig. 8*B* and data not shown).

Because activation of PLC-$\gamma$1 regulates T cell $Ca^{2+}$ signaling via inositol 1,4,5-triphosphate-dependent release of $Ca^{2+}$ from intracellular stores, we asked whether ezrin and moesin are required for $Ca^{2+}$ responses to TCR engagement. As shown in Fig. 8*C*, murine T cell blasts lacking both ezrin and moesin showed a significant decrease in both the magnitude and duration of $Ca^{2+}$ influx relative to control T cells, and cells lacking either ezrin or moesin alone showed intermediate $Ca^{2+}$ responses. Similar results were obtained using shRNA-mediated suppression of ezrin and moesin in Jurkat T cells (Fig. 8*F*), which show a more robust and uniform $Ca^{2+}$ response than the T cell blasts (Fig. 8*E*). In this experiment, T cells were stimulated with anti-CD3 Ab in the absence of extracellular $Ca^{2+}$ to monitor $Ca^{2+}$ store release. In comparison with control Jurkat T cells, ezrin- and moesin-suppressed Jurkat cells showed minimal store release, consistent with a defect at the level of inositol 1,4,5-triphosphate production by PLC-$\gamma$1. In keeping with this, treatment of ezrin/moesin double-deficient murine T cells with the SERCA pump inhibitor thapsigargin to induce $Ca^{2+}$ store release bypassed the defect in these cells (Fig. 8*D*).

To ask whether these defects in $Ca^{2+}$ signaling can account for the defects that we observe in IL-2 production, we measured activation of $Ca^{2+}$-dependent NF-AT elements within the IL-2 promoter. As shown in Fig. 8*G*, activation of NF-AT elements was significantly diminished in T cells suppressed for ezrin and moesin. This effect was specific to NF-AT, because activation of NF-$\kappa$B elements was unaffected. Taken together, these results show that ezrin and moesin work together to promote optimal PLC-$\gamma$1 activation and $Ca^{2+}$ signaling events leading to transcriptional activation of IL-2 gene expression.

## Discussion

Ezrin and moesin are important for numerous aspects of T cell function, but it has been unclear to what extent these closely related proteins serve unique roles. Many studies have treated ERM proteins indiscriminately or regarded moesin (the more abundant ERM protein in T cells) as functionally dominant; however, recent findings suggest that ezrin is uniquely required for T cell activation (30). We have conducted a systematic analysis of this question in primary murine T cells deficient for ezrin and/or moesin. We find that whereas ezrin and moesin can exhibit distinct behaviors in response to TCR engagement, they play overlapping functional roles in supporting T cell activation.

The literature is divided regarding how ERM proteins move in response to TCR engagement. Ezrin and moesin have been found to either localize together in the DPC (14, 15), or at opposite poles, with ezrin at the IS (45) and moesin at the DPC (30). Our findings suggest a resolution to this discrepancy. We show that at early times after TCR engagement, ezrin localizes to the IS, but at later times it moves to the DPC. Our previous data showing ezrin at the DPC were obtained after 20 min of engagement, a time when the DPC distribution predominates. In contrast, the studies conducted by Bretscher and coworkers (30) were largely performed at shorter time points, when the IS pattern is dominant. Our findings are supported by recent studies by the Tasken laboratory (46) using human peripheral blood T cells. They saw that ezrin colocalized initially with CD3 after stimulation with SEB-pulsed B cells, but at later times ezrin localized to the distal pole. We note that differential ERM movement occurs over the same timeframe as ERM dephosphorylation/rephosphorylation, although technical differences make it difficult to directly compare these studies. Nevertheless, our results suggest that at early times after TCR engagement, newly rephosphorylated ezrin and moesin associate with different binding partners in distinct domains of the plasma membrane.

Ezrin's transient movement to the IS suggests that it may play a unique role in TCR-mediated signaling events. In support of this idea, a recent study from the Bretscher

laboratory (30) showed that overexpression of ezrin mutants and siRNA-mediated suppression of ezrin in Jurkat T cells causes defects in IS formation, as defined by the failure to recruit ZAP70 to the site of TCR engagement. To ask about ezrin-specific aspects in T cell activation in greater detail, we generated mice with conditional deletion of ezrin in primary T cells. Our results show that ezrin-deficient T cells exhibit partial defects in IL-2 production, consistent with the view that ezrin is required for T cell activation. However, these cells formed a normal IS, as defined by recruitment and partitioning of the canonical markers PKC-$\theta$ and talin. Localization of phospho-ZAP70 confirmed that its recruitment to the IS occurred normally in these cells. Early tyrosine phosphorylation events occurred normally, including phosphorylation of ZAP70, an event that requires binding of ZAP70 to phosphorylated ITAMs with the TCR complex. Finally, we found that ezrin-deficient T cells undergo normal phosphorylation of PLC-$\gamma$1 and ERK1/2, and normal up-regulation of surface activation markers. We conclude that whereas ezrin does facilitate T cell activation, it is not required for signaling events at the IS. Indeed, ERM proteins generally appear to be dispensable for IS function, because no defects in IS organization were observed in cells expressing the ERM dominant-negative mutant (15), or in cells deficient for both ezrin and moesin.

The role of ERM proteins in organizing the DPC is well documented. We have identified three new DPC proteins, p85, CBP, and EBP50. Each of these proteins reportedly interacts preferentially with ezrin (37, 44), and each showed diminished DPC localization in ezrin-deficient cells. Nonetheless, a significant proportion of cells was still able to recruit these proteins to the DPC. This may reflect a residual ability of these proteins to interact with moesin. It is also likely that higher order interactions among DPC proteins (for example, those involving PDZ-domain proteins) foster the assembly of this complex. In an effort to distinguish between these possibilities, we developed an RNA interference-based strategy to suppress moesin expression in ezrin knockout T cells. Surprisingly, we found that even CD43, a protein for which ERM-dependent targeting to the DPC is well established, showed normal DPC localization in the double-deficient cells. We believe that this result reflects the inability of our RNA interference-based strategy to adequately deplete moesin expression. Although the T cell blasts used in these studies expressed only trace amounts of ezrin and radixin, they expressed moesin at 15–20% normal levels. Moreover, the residual moesin is hyperphosphorylated, indicating that the cells have maintained a significant pool of active, threonine-phosphorylated ERM proteins by recruiting additional molecules from the inactive cytoplasmic pool. For example, in the experiment shown in Fig. 7, suppression was efficient, but phospho-ERM levels were reduced by only 50%. This compensatory effect not only accounts for the modest phenotypes we observe, but also demonstrates that the T cells are under pressure to retain active ERM proteins.

Despite the pressure to retain ERM protein levels, T cell signaling is clearly perturbed by loss of ezrin and moesin. As with T cells lacking ezrin alone, T cells lacking moesin alone exhibited partial defects in IL-2 production and $Ca^{2+}$ signaling without obvious effects on other early signaling events. Significantly, these defects were more profound in cells deficient for both ezrin and moesin. Double-deficient cells showed defects in PLC-$\gamma$1 signaling that were usually too subtle to detect in single-deficient cells. The defects in $Ca^{2+}$ signaling in ezrin/moesin double-deficient T cells are largely attributable to defects in $Ca^{2+}$ store release, as evidenced by monitoring $Ca^{2+}$ elevation in the absence of exogenous $Ca^{2+}$. In support of this conclusion, pharmacological store depletion with thapsigargin bypassed the $Ca^{2+}$ defect in these cells. It remains possible that there are additional defects in coupling to $Ca^{2+}$ release activated $Ca^{2+}$ channels that are also bypassed by thapsigargin treatment. Taken together, our results show that ezrin and moesin are both important for PLC-$\gamma$1-dependent $Ca^{2+}$ signaling events leading to activation of NF-AT elements within the IL-2 promoter. Our results are best explained by a requirement for a certain overall expression

level of total ERM proteins. In this context, it is important to point out that given the high residual levels of phospho-moesin, the partial defects we observe in double-deficient T cells are likely to represent an underestimate of the requirement for ezrin and moesin in T cell signaling.

The mechanism by which ezrin and moesin impact PLC-$\gamma$1 phosphorylation remains to be elucidated. One possibility is that both ezrin and moesin contribute to activation of ZAP70 at the IS. We sometimes observed diminished ZAP70 phosphorylation in double-deficient cells; however, this result was not consistent, and recruitment of pZAP70 to the IS was intact. Alternatively, ezrin and moesin may be required to sequester a negative regulatory phosphatase at the DPC. In this context, SHP-1 is an excellent candidate, because localization of SHP-1 to the IS leads to diminished phosphorylation of multiple early T cell signaling intermediates, including PLC-$\gamma$1 (47–50). We now show that SHP-1 is a DPC component. SHP-1 localization to the DPC is intact in ezrin-deficient cells, but is dislocalized by overexpression of the ERM dominant-negative mutant (P. Cullinan and J. Burkhardt, unpublished data). Understanding how the DPC regulates the function of SHP-1 and other phosphatases will be an important area of future investigation.

Although our data show that ezrin and moesin play largely redundant roles in T cell activation, the unique behaviors of ezrin are striking and may yet prove to be functionally significant. We show that TCR engagement results in tyrosine phosphorylation of ezrin at tyrosines 146 and 353, functionally important sites in nonhematopoietic cells (37–40). The relevant kinase in T cells remains to be identified; however, Lck is required for ezrin tyrosine phosphorylation, and Lck can phosphorylate ezrin at tyrosine 146 in vitro (51–53). Interestingly, we find that ezrin, but not moesin, can interact with the SH2 domain of Lck in vitro. Although it remains to be demonstrated that ezrin binds to Lck in T cells, any direct interaction between these proteins most likely occurs early after TCR stimulation, when both molecules are localized to the IS.

In addition to their function in TCR signaling, ezrin and moesin participate in several other T cell signaling pathways, including polarity, apoptosis, and cell migration (1). In each of these contexts, it will be important to revisit the question of unique vs redundant functions. Through the use of T cells deficient for specific ERM proteins, it is now possible to move forward in understanding how these important proteins control T cell signaling and function.

## Acknowledgments

We thank Drs. Patrick Cullinan, Anne Sperling, Judy Cannon, Sarah Russell, Paula Oliver, and Yair Argon, as well as members of the Burkhardt laboratory for helpful discussions.

## References

1. Burkhardt JK, Carrizosa E, Shaffer MH. The actin cytoskeleton in T cell activation. Annu Rev Immunol. 2007; 26:233–259. [PubMed: 18304005]
2. Krummel MF, Macara I. Maintenance and modulation of T cell polarity. Nat Immunol. 2006; 7:1143–1149. [PubMed: 17053799]
3. Billadeau DD, Nolz JC, Gomez TS. Regulation of T-cell activation by the cytoskeleton. Nat Rev Immunol. 2007; 7:131–143. [PubMed: 17259969]
4. Yokosuka T, Sakata-Sogawa K, Kobayashi W, Hiroshima M, Hashimoto-Tane A, Tokunaga M, Dustin ML, Saito T. Newly generated T cell receptor microclusters initiate and sustain T cell activation by recruitment of Zap70 and SLP-76. Nat Immunol. 2005; 6:1253–1262. [PubMed: 16273097]

5. Varma R, Campi G, Yokosuka T, Saito T, Dustin ML. T cell receptor-proximal signals are sustained in peripheral microclusters and terminated in the central supramolecular activation cluster. Immunity. 2006; 25:117–127. [PubMed: 16860761]
6. Bunnell SC, Hong DI, Kardon JR, Yamazaki T, McGlade CJ, Barr VA, Samelson LE. T cell receptor ligation induces the formation of dynamically regulated signaling assemblies. J Cell Biol. 2002; 158:1263–1275. [PubMed: 12356870]
7. Campi G, Varma R, Dustin ML. Actin and agonist MHC-peptide complex-dependent T cell receptor microclusters as scaffolds for signaling. J Exp Med. 2005; 202:1031–1036. [PubMed: 16216891]
8. Ryser JE, Rungger-Brandle E, Chaponnier C, Gabbiani G, Vassalli P. The area of attachment of cytotoxic T lymphocytes to their target cells shows high motility and polarization of actin, but not myosin. J Immunol. 1982; 128:1159–1162. [PubMed: 7035558]
9. Chang JT V, Palanivel R, Kinjyo I, Schambach F, Intlekofer AM, Banerjee A, Longworth SA, Vinup KE, Mrass P, Oliaro J, et al. Asymmetric T lymphocyte division in the initiation of adaptive immune responses. Science. 2007; 315:1687–1691. [PubMed: 17332376]
10. Ludford-Menting MJ, Oliaro J, Sacirbegovic F, Cheah ET, Pedersen N, Thomas SJ, Pasam A, Iazzolino R, Dow LE, Waterhouse NJ, et al. A network of PDZ-containing proteins regulates T cell polarity and morphology during migration and immunological synapse formation. Immunity. 2005; 22:737–748. [PubMed: 15963788]
11. Ivetic A, Ridley AJ. Ezrin/Radixin/Moesin proteins and Rho GTPase signalling in leukocytes. Immunology. 2004; 112:165–176. [PubMed: 15147559]
12. Bretscher A, Edwards K, Fehon RG. ERM proteins and merlin: integrators at the cell cortex. Nat Rev Mol Cell Biol. 2002; 3:586–599. [PubMed: 12154370]
13. Yonemura S, Hirao M, Doi Y, Takahashi N, Kondo T, Tsukita S, Tsukita S. Ezrin/Radixin/Moesin (ERM) proteins bind to a positively charged amino acid cluster in the juxta-membrane cytoplasmic domain of CD44, CD43, and ICAM-2. J Cell Biol. 1998; 140:885–895. [PubMed: 9472040]
14. Delon J, Kaibuchi K, Germain RN. Exclusion of CD43 from the immunological synapse is mediated by phosphorylation-regulated relocation of the cytoskeletal adaptor moesin. Immunity. 2001; 15:691–701. [PubMed: 11728332]
15. Allenspach EJ, Cullinan P, Tong J, Tang Q, Tesciuba AG, Cannon JL, Takahashi SM, Morgan R, Burkhardt JK, Sperling AI. ERM-dependent movement of CD43 defines a novel protein complex distal to the immunological synapse. Immunity. 2001; 15:739–750. [PubMed: 11728336]
16. Cullinan P, Sperling AI, Burkhardt JK. The distal pole complex: a novel membrane domain distal to the immunological synapse. Immunol Rev. 2002; 189:111–122. [PubMed: 12445269]
17. Li Q, Nance MR, Kulikauskas R, Nyberg K, Fehon R, Karplus PA, Bretscher A, Tesmer JJ. Self-masking in an intact ERM-merlin protein: an active role for the central $\alpha$-helical domain. J Mol Biol. 2007; 365:1446–1459. [PubMed: 17134719]
18. Fievet BT, Gautreau A, Roy C, Del Maestro L, Mangeat P, Louvard D, Arpin M. Phosphoinositide binding and phosphorylation act sequentially in the activation mechanism of ezrin. J Cell Biol. 2004; 164:653–659. [PubMed: 14993232]
19. Simons PC, Pietromonaco SF, Reczek D, Bretscher A, Elias L. C-terminal threonine phosphorylation activates ERM proteins to link the cell's cortical lipid bilayer to the cytoskeleton. Biochem Biophys Res Commun. 1998; 253:561–565. [PubMed: 9918767]
20. Matsui T, Maeda M, Doi Y, Yonemura S, Amano M, Kaibuchi K, Tsukita S, Tsukita S. Rho-kinase phosphorylates COOH-terminal threonines of ezrin/radixin/moesin (ERM) proteins and regulates their head-to-tail association. J Cell Biol. 1998; 140:647–657. [PubMed: 9456324]
21. Faure S, Salazar-Fontana LI, Semichon M, Tybulewicz VL, Bismuth G, Trautmann A, Germain RN, Delon J. ERM proteins regulate cytoskeleton relaxation promoting T cell-APC conjugation. Nat Immunol. 2004; 5:272–279. [PubMed: 14758359]
22. Brown MJ, Nijhara R, Hallam JA, Gignac M, Yamada KM, Erlandsen SL, Delon J, Kruhlak M, Shaw S. Chemokine stimulation of human peripheral blood T lymphocytes induces rapid dephosphorylation of ERM proteins, which facilitates loss of microvilli and polarization. Blood. 2003; 102:3890–3899. [PubMed: 12907449]

23. Stewart MP, McDowall A, Hogg N. LFA-1-mediated adhesion is regulated by cytoskeletal restraint and by a $Ca^{2+}$-dependent protease, calpain. J Cell Biol. 1998; 140:699–707. [PubMed: 9456328]
24. Bleijs DA, van Duijnhoven GC, van Vliet SJ, Thijssen JP, Figdor CG, van Kooyk Y. A single amino acid in the cytoplasmic domain of the $\beta_2$ integrin lymphocyte function-associated antigen-1 regulates avidity-dependent inside-out signaling. J Biol Chem. 2001; 276:10338–10346. [PubMed: 11134023]
25. Bretscher A. Regulation of cortical structure by the ezrin-radixin-moesin protein family. Curr Opin Cell Biol. 1999; 11:109–116. [PubMed: 10047517]
26. Doi Y, Itoh M, Yonemura S, Ishihara S, Takano H, Noda T, Tsukita S. Normal development of mice and unimpaired cell adhesion/cell motility/actin-based cytoskeleton without compensatory up-regulation of ezrin or radixin in moesin gene knockout. J Biol Chem. 1999; 274:2315–2321. [PubMed: 9890997]
27. Kikuchi S, Hata M, Fukumoto K, Yamane Y, Matsui T, Tamura A, Yonemura S, Yamagishi H, Keppler D, Tsukita S, Tsukita S. Radixin deficiency causes conjugated hyperbilirubinemia with loss of Mrp2 from bile canalicular membranes. Nat Genet. 2002; 31:320–325. [PubMed: 12068294]
28. Saotome I, Curto M, McClatchey AI. Ezrin is essential for epithelial organization and villus morphogenesis in the developing intestine. Dev Cell. 2004; 6:855–864. [PubMed: 15177033]
29. Bonilha VL, Rayborn ME, Saotome I, McClatchey AI, Hollyfield JG. Microvilli defects in retinas of ezrin knockout mice. Exp Eye Res. 2006; 82:720–729. [PubMed: 16289046]
30. Ilani T, Khanna C, Zhou M, Veenstra TD, Bretscher A. Immune synapse formation requires ZAP-70 recruitment by ezrin and CD43 removal by moesin. J Cell Biol. 2007; 179:733–746. [PubMed: 18025306]
31. Shcherbina A, Bretscher A, Kenney DM, Remold-O'Donnell E. Moesin, the major ERM protein of lymphocytes and platelets, differs from ezrin in its insensitivity to calpain. FEBS Lett. 1999; 443:31–36. [PubMed: 9928947]
32. Kaye J, Hsu ML, Sauron ME, Jameson SC, Gascoigne NR, Hedrick SM. Selective development of $CD4^+$ T cells in transgenic mice expressing a class II MHC-restricted antigen receptor. Nature. 1989; 341:746–749. [PubMed: 2571940]
33. Gomez TS, Hamann MJ, McCarney S, Savoy DN, Lubking CM, Heldebrant MP, Labno CM, McKean DJ, McNiven MA, Burkhardt JK, Billadeau DD. Dynamin 2 regulates T cell activation by controlling actin polymerization at the immunological synapse. Nat Immunol. 2005; 6:261–270. [PubMed: 15696170]
34. Nolz JC, Gomez TS, Zhu P, Li S, Medeiros RB, Shimizu Y, Burkhardt JK, Freedman BD, Billadeau DD. The WAVE2 complex regulates actin cytoskeletal reorganization and CRAC-mediated calcium entry during T cell activation. Curr Biol. 2006; 16:24–34. [PubMed: 16401421]
35. Cannon JL, Labno CM, Bosco G, Seth A, McGavin MH, Siminovitch KA, Rosen MK, Burkhardt JK. Wasp recruitment to the T cell:APC contact site occurs independently of Cdc42 activation. Immunity. 2001; 15:249–259. [PubMed: 11520460]
36. Egerton M, Burgess WH, Chen D, Druker BJ, Bretscher A, Samelson LE. Identification of ezrin as an 81-kDa tyrosine-phosphorylated protein in T cells. J Immunol. 1992; 149:1847–1852. [PubMed: 1381389]
37. Gautreau A, Poullet P, Louvard D, Arpin M. Ezrin, a plasma membrane-microfilament linker, signals cell survival through the phosphatidylinositol 3-kinase/Akt pathway. Proc Natl Acad Sci USA. 1999; 96:7300–7305. [PubMed: 10377409]
38. Srivastava J, Elliott BE, Louvard D, Arpin M. Src-dependent ezrin phosphorylation in adhesion-mediated signaling. Mol Biol Cell. 2005; 16:1481–1490. [PubMed: 15647376]
39. Crepaldi T, Gautreau A, Comoglio PM, Louvard D, Arpin M. Ezrin is an effector of hepatocyte growth factor-mediated migration and morphogenesis in epithelial cells. J Cell Biol. 1997; 138:423–434. [PubMed: 9230083]
40. Krieg J, Hunter T. Identification of the two major epidermal growth factor-induced tyrosine phosphorylation sites in the microvillar core protein ezrin. J Biol Chem. 1992; 267:19258–19265. [PubMed: 1382070]

41. Lee PP, Fitzpatrick DR, Beard C, Jessup HK, Lehar S, Makar KW, Perez-Melgosa M, Sweetser MT, Schlissel MS, Nguyen S, et al. A critical role for Dnmt1 and DNA methylation in T cell development, function, and survival. Immunity. 2001; 15:763–774. [PubMed: 11728338]
42. Finkelstein LD, Shimizu Y, Schwartzberg PL. Tec kinases regulate TCR-mediated recruitment of signaling molecules and integrin-dependent cell adhesion. J Immunol. 2005; 175:5923–5930. [PubMed: 16237085]
43. Takahashi K, Sasaki T, Mammoto A, Takaishi K, Kameyama T, Tsukita S, Takai Y. Direct interaction of the Rho GDP dissociation inhibitor with ezrin/radixin/moesin initiates the activation of the Rho small G protein. J Biol Chem. 1997; 272:23371–23375. [PubMed: 9287351]
44. Itoh K, Sakakibara M, Yamasaki S, Takeuchi A, Arase H, Miyazaki M, Nakajima N, Okada M, Saito T. Cutting edge: negative regulation of immune synapse formation by anchoring lipid raft to cytoskeleton through Cbp-EBP50-ERM assembly. J Immunol. 2002; 168:541–544. [PubMed: 11777944]
45. Roumier A, Olivo-Marin JC, Arpin M, Michel F, Martin M, Mangeat P, Acuto O, Dautry-Varsat A, Alcover A. The membrane-microfilament linker ezrin is involved in the formation of the immunological synapse and in T cell activation. Immunity. 2001; 15:715–728. [PubMed: 11728334]
46. Ruppelt A, Mosenden R, Gronholm M, Aandahl EM, Tobin D, Carlson CR, Abrahamsen H, Herberg FW, Carpen O, Tasken K. Inhibition of T cell activation by cyclic adenosine 5′-monophosphate requires lipid raft targeting of protein kinase A type I by the A-kinase anchoring protein ezrin. J Immunol. 2007; 179:5159–5168. [PubMed: 17911601]
47. Monu N, Frey AB. Suppression of proximal T cell receptor signaling and lytic function in $CD8^+$ tumor-infiltrating T cells. Cancer Res. 2007; 67:11447–11454. [PubMed: 18056473]
48. Stefanova I, Hemmer B, Vergelli M, Martin R, Biddison WE, Germain RN. TCR ligand discrimination is enforced by competing ERK positive and SHP-1 negative feedback pathways. Nat Immunol. 2003; 4:248–254. [PubMed: 12577055]
49. Stebbins CC, Watzl C, Billadeau DD, Leibson PJ, Burshtyn DN, Long EO. Vav1 dephosphorylation by the tyrosine phosphatase SHP-1 as a mechanism for inhibition of cellular cytotoxicity. Mol Cell Biol. 2003; 23:6291–6299. [PubMed: 12917349]
50. Kosugi A, Sakakura J, Yasuda K, Ogata M, Hamaoka T. Involvement of SHP-1 tyrosine phosphatase in TCR-mediated signaling pathways in lipid rafts. Immunity. 2001; 14:669–680. [PubMed: 11420038]
51. Tomas EM, Darlington PJ, Chau LA, Madrenas J. The role of ezrin in T-cell receptor-dependent signaling. Transplant Proc. 2001; 33:207–208. [PubMed: 11266781]
52. Thuillier L, Hivroz C, Fagard R, Andreoli C, Mangeat P. Ligation of CD4 surface antigen induces rapid tyrosine phosphorylation of the cytoskeletal protein ezrin. Cell Immunol. 1994; 156:322–331. [PubMed: 8025951]
53. Autero M, Heiska L, Ronnstrand L, Vaheri A, Gahmberg CG, Carpen O. Ezrin is a substrate for Lck in T cells. FEBS Lett. 2003; 535:82–86. [PubMed: 12560083]

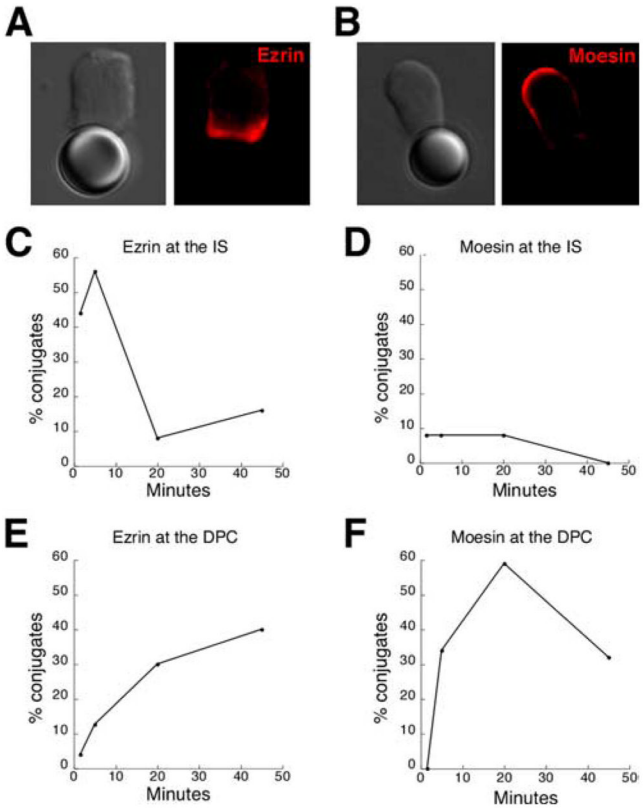


**FIGURE 1.**

Ezrin localizes transiently to the IS, whereas moesin moves directly to the DPC. Purified naive mouse T cells were conjugated with anti-TCR$\beta$/CD28-coated beads for various times, and conjugates were fixed and fluorescently labeled with anti-ezrin or anti-moesin Abs. Ezrin (*A*) and moesin (*B*) localization at 1.5 min. *C–F*, Conjugates fixed at the indicated times were selected randomly, and the distribution of ezrin or moesin was scored with respect to the IS (defined as enrichment at the cell/bead contact site), exemplified in *A*, or the DPC (defined as exclusion from the site of cell/bead contact area or capping at the distal T cell pole), exemplified in *B*. The percentage of conjugates showing each pattern was calculated as a function of total T cell/bead conjugates. Note that although IS and DPC distributions are reciprocal, the scoring does not sum to 100% because some T cells exhibited neither pattern. At least 50 conjugates were scored for each time point in each of three independent experiments; results are from one representative experiment.

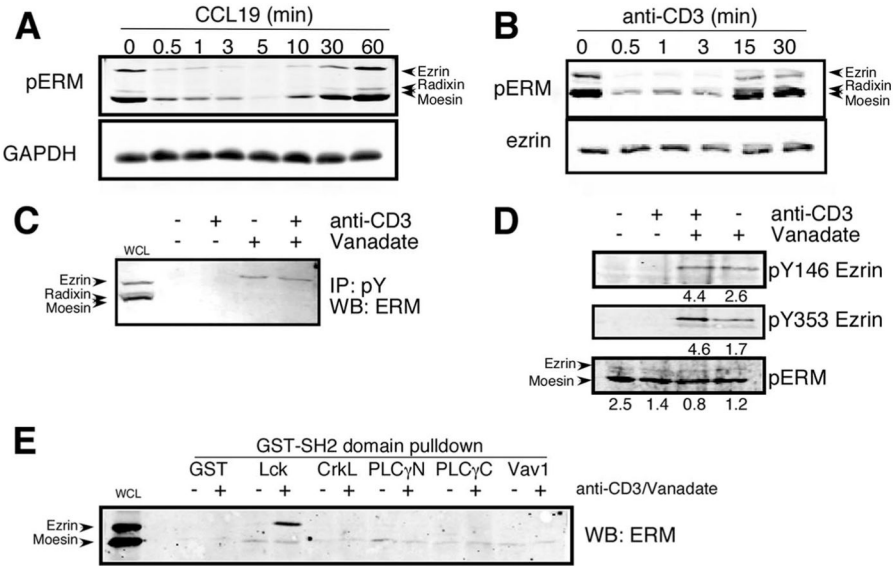


**FIGURE 2.**

Ezrin and moesin differ with respect to tyrosine, but not threonine, phosphorylation in T cells. *A*, T cells were stimulated for the indicated times with CCL19, and whole-cell lysates were immunoblotted with anti-pT-ERM Ab, which detects the activated form of all three ERM proteins. *B*, T cells were stimulated for the indicated times by CD3 cross-linking, and threonine phosphorylation was analyzed as in *A*. *C*, To assess overall tyrosine phosphorylation, T cells were stimulated by CD3 cross-linking in the presence or absence of vanadate. ERM proteins were then immunoprecipitated using a mixture of anti-phosphotyrosine Abs and immunoblotted with anti-total ERM Ab. *D*, To test known phosphorylation sites, T cells were stimulated as in *C*, and whole-cell lysates were immunoblotted with the indicated phospho-specific Abs. Numbers indicate arbitrary fluorescence units for each band. All results were similar regardless of whether naive (*B* and *D*) or previously activated (*A* and *C*) T cells were used (data not shown). *E*, Jurkat T cells were stimulated with anti-CD3 Ab and vanadate, and lysates were subjected to affinity purification using a panel of rGST SH2-domain fusion proteins. Bound proteins were immunoblotted with an Ab that recognizes all ERM proteins.

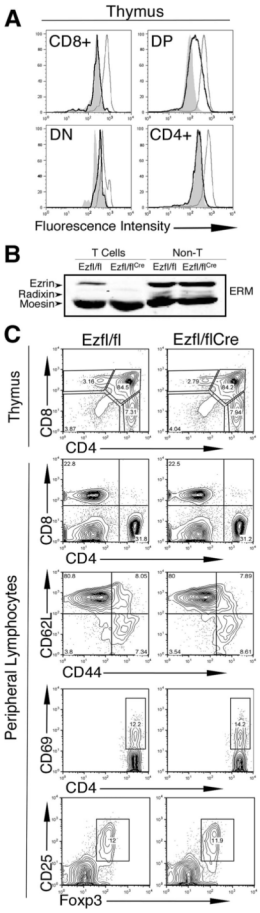


**FIGURE 3.**

Conditional deletion of ezrin in double-positive T cells results in normal T cell development. *A*, Thymocytes from ezrin$^{flox/flox}$ or ezrin$^{flox/flox:CD4Cre}$ mice were surface labeled for CD4 and CD8, then fixed and labeled intracellularly with anti-ezrin or control IgG Ab. Light line, ezrin$^{flox/flox}$; bold line, ezrin$^{flox/flox:CD4Cre}$; filled line, IgG control. *B*, Lymphocytes from ezrin$^{flox/flox}$ or ezrin$^{flox/flox:CD4Cre}$ mice were enriched or depleted for T cells, as described in *Materials and Methods*. Lysates were immunoblotted with anti-total ERM Ab. *C*, Total thymocytes or lymph node lymphocytes from ezrin$^{flox/flox}$ or ezrin$^{flox/flox:CD4Cre}$ mice were analyzed by flow cytometry using the indicated Abs.

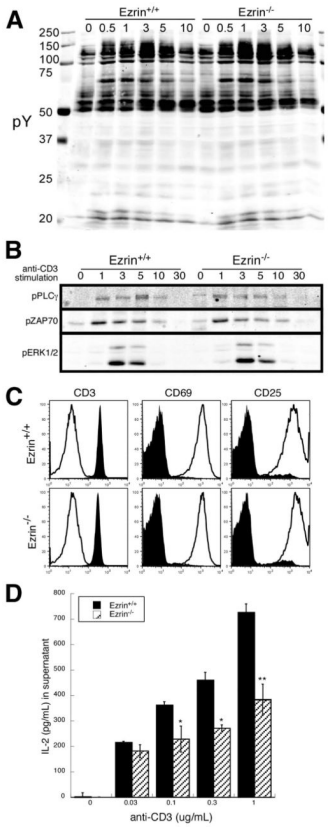


**FIGURE 4.**

Ezrin$^{-/-}$ T cells exhibit normal proximal TCR signaling, but fail to make normal levels of IL-2. Naive CD4$^{+}$ T cells purified from ezrin$^{flox/flox}$ or ezrin$^{flox/flox:CD4Cre}$ mice were stimulated with anti-CD3-biotin plus streptavidin for the indicated times, lysed, and immuno-blotted for total pY (*A*) or pPLC-$\gamma$1, pZAP70, and pERK (*B*). Alternatively, purified T cells were stimulated for 24 h with 1 $\mu$g/ml anti-CD3 plus T-depleted splenocytes (open histograms) or with T-depleted splenocytes alone (closed histograms), and surface levels of CD3, CD25, and CD69 were assessed by flow cytometry (*C*). *D*, Supernatants from cells stimulated as in *C* were analyzed for IL-2 by ELISA. **, $p \leq 0.01$; *, $p \leq 0.05$.

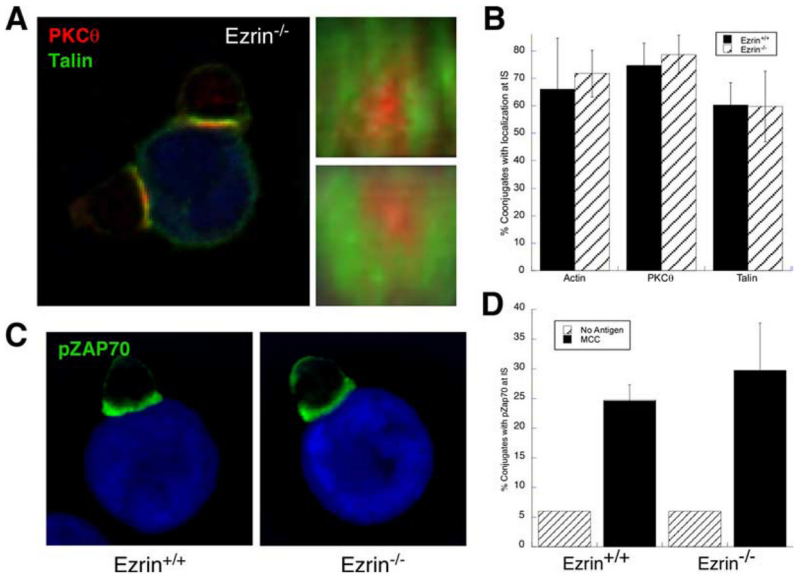


**FIGURE 5.**

Ezrin$^{-/-}$ T cells exhibit normal IS formation. Purified ezrin$^{-/-}$ and ezrin$^{+/+}$ AND TCR Tg T cells were conjugated to $MCC_{88–103}$-pulsed (or unpulsed) CH27 B cells for 3 min, and conjugates were fixed and fluorescently labeled with Abs to PKC-$\theta$, talin, pZAP70, and rhodamine-phalloidin to label F-actin. Z-stack images were collected, and IS architecture was assessed using deconvolution and volume rendering. *A*, Representative conjugate containing one MCC-pulsed B cell (blue) and two ezrin$^{-/-}$ T cells, labeled for the canonical IS markers PKC-$\theta$ (red) and talin (green). *Right panels* in *A*, en face projections of the two cell-cell contact sites show focusing of PKC-$\theta$ within the central region (central supramolecular activation cluster) and talin accumulation in a peripheral ring (peripheral supramolecular activation cluster). Ezrin$^{+/+}$ T cells analyzed in parallel showed the same morphology (data not shown). *B*, Conjugates formed with peptide-pulsed B cells were selected at random and scored for the localization of F-actin, PKC-$\theta$, or talin to the IS. *C*, Conjugates formed with peptide-pulsed B cells were labeled with anti-pZAP70 to detect IS accumulation of the active form of the molecule. *D*, Conjugates formed as in *C* were selected at random and scored for the localization of pZAP70. *B* and *D*, At least 50 conjugates were scored for each condition; results are averages of at least three experiments ± SD.

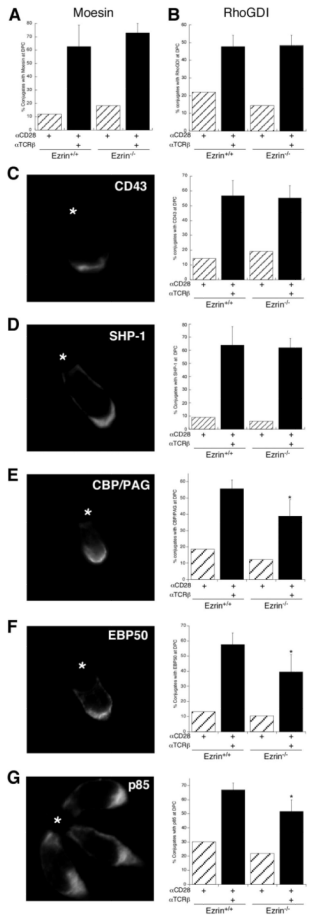


**FIGURE 6.**

Many DPC proteins localize normally in ezrin$^{-/-}$ T cells, but a newly identified subset is partially perturbed. Purified CD4$^{+}$ ezrin$^{+/+}$ and ezrin$^{-/-}$ mouse T cells were conjugated for 20 min with beads coupled to anti-TCR/CD28 or anti-CD28 alone (marked with *). Conjugates were fixed and stained with Abs for the indicated proteins, and localization of each protein to the DPC was scored. The established DPC markers moesin (*A*), RhoGDI (*B*), and CD43 (*C*) were unaffected by loss of ezrin expression. SHP-1 (*D*), a novel DPC protein, was also unaffected. In contrast, CBP/PAG (*E*), EBP50 (*F*), and p85 (*G*), proteins that bind preferentially to ezrin, all showed diminished DPC localization in ezrin$^{-/-}$ T cells. At least 50 conjugates were scored for each condition; results are averages of at least three experiments, ±SD. *, $p \leq 0.05$.

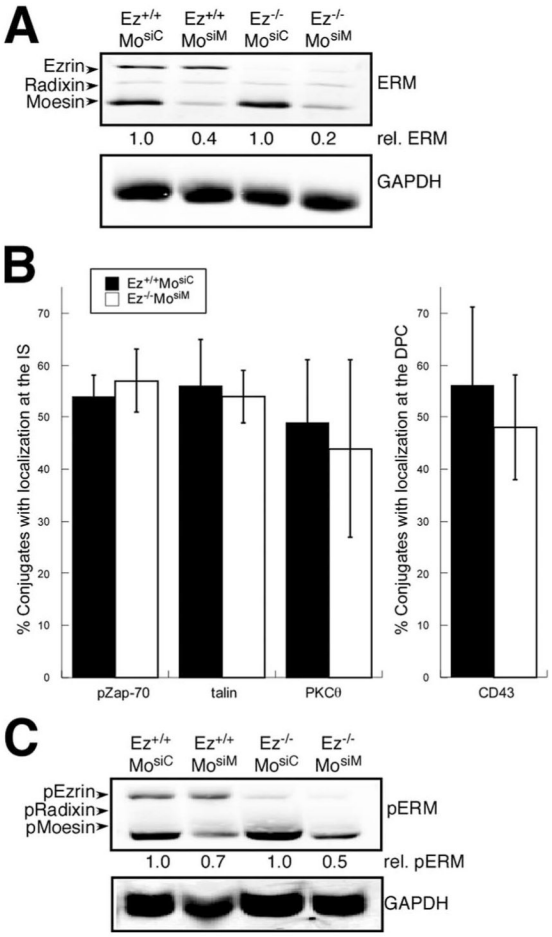


**FIGURE 7.**

Suppression of moesin in ezrin$^{-/-}$ T cells. Wild-type or ezrin$^{-/-}$ T cell blasts were transfected with control or moesin-specific siRNAs, to generate T cells deficient for ezrin alone, moesin alone, or both. *A*, Cells were lysed 48 h after transfection and immunoblotted with anti-total ERM Ab. Blotting with GAPDH was used as a loading control. Numbers indicate total ERM levels, relative to control cells. *B*, T cells prepared as in *A* were allowed to form conjugates with anti-TCR$\beta$-coated beads for 3 min (*left*) or 20 min (*right*), and polarization of the indicated IS and DPC markers was assessed by immunofluorescence microscopy. At least 50 conjugates were scored for each condition; results are averages of three experiments, ±SD. *C*, T cells prepared as in *A* were lysed and immunoblotted with anti-pT-ERM Ab. Numbers indicate total pT-ERM levels, relative to control cells. Note that whereas total ERM proteins are reduced by 80%, compensatory phosphorylation of moesin results in a net loss of only 50% of the active, phosphorylated pool of ERM proteins.

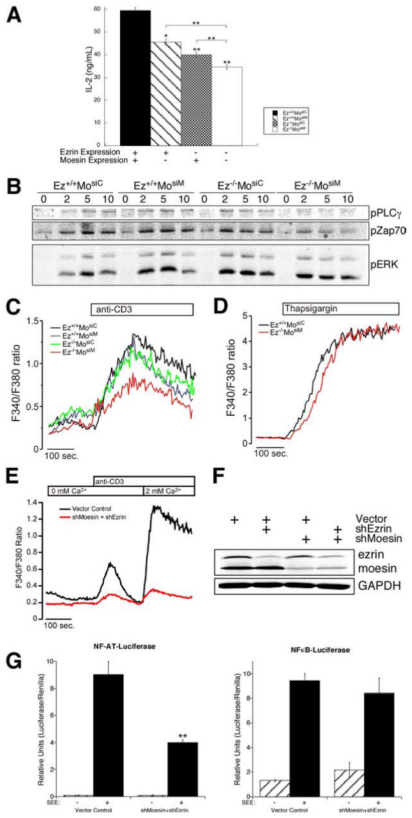


**FIGURE 8.**

Ezrin and moesin both contribute to T cell activation. *A–D*, Wild-type or ezrin$^{-/-}$ murine T cell blasts were transfected with control or moesin-specific siRNAs, to generate T cells deficient for ezrin alone, moesin alone, or both. *A*, IL-2 expression was determined by restimulation with plate-bound anti-CD3 and anti-CD28 Abs for 24 h, and analysis of cell supernatants by ELISA. *B*, Ezrin- and/or moesin-deficient T cell blasts were stimulated with soluble biotinylated anti-CD3 Ab and streptavidin for the indicated times at 37°C. Cells were lysed and immunoblotted with indicated phospho-specific Abs. *C* and *D*, To assess $Ca^{2+}$ responses, T cell blasts were pulsed with fura 2-AM and imaged in response to TCR cross-linking (*C*) or thapsigargin (*D*). *E*, Jurkat T cells were transfected with ezrin-and moesin-targeted shRNAs or with empty targeting vector. After 72 h, cells were loaded with fura 2-AM and imaged initially in medium lacking $Ca^{2+}$ to visualize release of $Ca^{2+}$ from intracellular stores. After stimulation with anti-CD3 Ab, cells were perfused with medium containing 2 mM $Ca^{2+}$ to visualize $Ca^{2+}$ release activated $Ca^{2+}$ channel-dependent $Ca^{2+}$ influx. *F*, Lysates from shRNA-transfected Jurkat T cells shown in *E* were immunoblotted with Abs against ezrin, moesin, and GAPDH. *G*, Jurkat T cells were transfected with ezrin- and moesin-targeted shRNAs or with empty targeting vector, together with the indicated luciferase reporter plasmids and TK *Renilla*. Cells were stimulated by mixing with Raji B cells in the presence or absence of staphylococcal enterotoxin E, and luciferase activity was assessed after 7 h of coculture. Values were normalized to *Renilla* activity, and represent means ± SD of quadruplicate samples. **, $p < 0.01$.